Adsorption of Organic Friction Modifier Additives

Benjamin M. Fry[1], Gareth Moody[2], Hugh A. Spikes[1] and Janet S. S. Wong[1†]

[1] Department of Mechanical Engineering, Imperial College London, London SW7 2AZ, UK.

[2] Croda Lubricants, Croda Europe Ltd, Cowick Hall, Snaith, East Yorkshire, DN14 9AA, UK.

[†] Corresponding author j.wong@imperial.ac.uk

ABSTRACT

Organic friction modifier additives (OFMs) are surfactant molecules added to engine oils to reduce friction in the boundary lubrication regime. They are thought to work by forming an absorbed layer which provides low friction. This paper studied the relationship between the adsorption of OFMs and their friction and wear reducing properties in a rubbing contact formed by a stationary glass ball and a rotating silicon disk under the boundary lubrication regime. The effect of molecular structure was investigated by using OFMs of various tail saturation and head group chemistry. OFM tested were oleic acid, octadecylamine, oleylamine and glycerol monooleate.

The thickness of an OFM adsorbed layer in hexadecane, examined in-situ by spectroscopic ellipsometry and quartz crystal microbalance (QCM), depends on the molecular structure and the concentration of the OFM. As expected, saturated, linear chain gives the thickest film. A critical OFM layer thickness of about 0.6 nm is necessary to achieve low initial and maximum friction. The thicker OFM layers are accompanied by narrower wear tracks, which are rougher than the wider, smoother wear tracks formed with thinner OFM layers. The interplay between the thickness of the OFM layer and wear track surface roughness results in all OFM layers having similar steady friction. This shows that the apparent effect of OFM depends on the stage of rubbing test: initially on friction; and then subsequently on surface damage.

Despite OFMs and the base oil having similar refractive indices, ellipsometry was found to be a suitable technique for examining the adsorption of OFM additives from an oil based solution, and showed reasonable correlation with QCM results.

INTRODUCTION

Organic friction modifiers (OFMs) are amphiphilic surfactant molecules that adsorb to solid surfaces through their polar headgroups.[1] Since the early 1920s,[2,3] it has been widely accepted that when OFMs are added to lubricants, they form close-packed self-assembled monolayers (SAMs) on the sliding surfaces which prevent asperity contact and thus significantly reduces friction and wear.[1]

The tribological properties of SAMs have been widely studied. By keeping the average area per molecule constant (21.6 $Å^2$/molecule for thiols on gold [4]), changing the length of the tail group of a thiol results in a change in friction on gold surface in air, as measured through friction force microscopy (FFM). Below a critical chain length of C12, friction is high. Further increase in chain length however has a minimal effect on friction. This critical chain length was said to be linked to the van der Waals force among tail chains in the monolayer, above which the force was sufficient to prevent the formation of gauche defects which causes an increase in friction. [5]

The density of the tail groups of thiols on gold can be changed by using thiols of different molecular structures (1 head group, 1 tail group; 2 head groups, 1 tail group; 2 head groups and 2 tail groups), resulting in a packing density of 21.6-33.75 $Å^2$/molecule. It was found that a less densely packed layer has a higher friction.[6] Packing density has also been shown to be linked to the molecular tilt. The larger the tilt as observed in a more sparsely packed layer, the less the van der Waals forces are in the monolayer.[7] Both of these factors change the height of the monolayer, and the friction.

Some of the findings about thiol described above apply to OFMs adsorbed from a solution onto a surface. The effect of the tail length of OFM additives was studied by Hardy which found that a C12 chain was needed to achieve low friction.[8] Jahanmir however later concluded that the optimum OFM tail length depends on the test conditions.[9] The effect of chain packing observed with thiol is not as clear with OFM molecules. Previous quartz crystal microbalance (QCM) measurements showed that the packing density of oleic acid on steel coated QCM crystals was 100 Å^2/molecule.[10] Various amine based friction modifiers have also been shown to have an adsorption density of over 100 Å^2/molecule.[11] This suggests that OFM molecules are significantly more loosely packed than a thiol monolayer.

Molecular dynamics (MD) simulations of OFMs adsorbed on iron and iron oxide surfaces have shown that a higher surface coverage leads to lower friction[12–15]. A recent combined experimental and simulation study has suggested that, although friction decreases with increasing OFM coverage, complete coverage of the surface is not necessary for an effective friction reduction.[16] This has been suggested that surface coverage may have a stronger effect than tail length on friction of OFMs. This is because the thickness of the OFM layer may change during rubbing. The height of a palmitic acid layer in hexadecane on a copper surface has been shown using frequency modulated atomic force microscopy (FM-AFM) to grow from 2.5 nm to about 20 nm during continuous scanning.[17] Polarised neutron reflectometry (PNR) showed that the adsorbed film had an initial thickness of 1.4 nm, which then formed a multilayer (reaches 5.9 nm) when under a constant pressure of 3MPa.[18] Colloidal probe AFM measurements (with a Hertzian maximum pressure of 210 MPa) of a palmitic acid layer on copper showed a reduction in friction without a change in layer thickness within a pre-scratched area.[18] They suggested that rubbing may change the additive layer other than its height.

While intuitively the adsorption of OFM additives should play a significant role in friction properties of OFM layers, there is increasing evidence showing that the OFM layers may

change during rubbing. This poses the question of whether the importance of adsorption behaviour of OFMs on friction remains as rubbing progresses. The aim of this research is to study the relationship between the adsorption and the friction reducing properties of OFM additives at the initial rubbing stage and when steady state friction coefficient is established. In this work, two in-situ techniques were used to measure the adsorption of the OFM additives on silicon; QCM, which has previously been shown to measure the adsorbed mass of OFM molecules;[19,20] and spectroscopic ellipsometry, a technique which is used for oil based adsorption measurements for the first time. These results were correlated to the friction reduction properties of OFM in the boundary friction regime.

MATERIALS

Four OFM additives (see their molecular structures in Figure 1) were chosen to examine the effects of surface-OFM interactions and tail structures of OFM on the tribological performance of OFMs. They were octadecylamine, oleylamine, oleic acid and glycerol monooleate. All were ≥99% in purity, purchased from Sigma Aldrich and used as received. The base oil was hexadecane (99%, Sigma Aldrich) which was cleaned through a column containing activated alumina, silica gel and 3 Å molecular sieves (all bought from Sigma Aldrich). 1 mM solutions were prepared by stirring OFMs in cleaned hexadecane at 60 °C for 2 hours. These corresponded to w/w 0.035%, 0.035%, 0.037% and 0.046% for octadecylamine, oleylamine, oleic acid and glycerol monooleate respectively. 0.1 mM and 10 mM oleylamine solutions (w/w 0.0035% and 0.35% respectively) were also prepared.

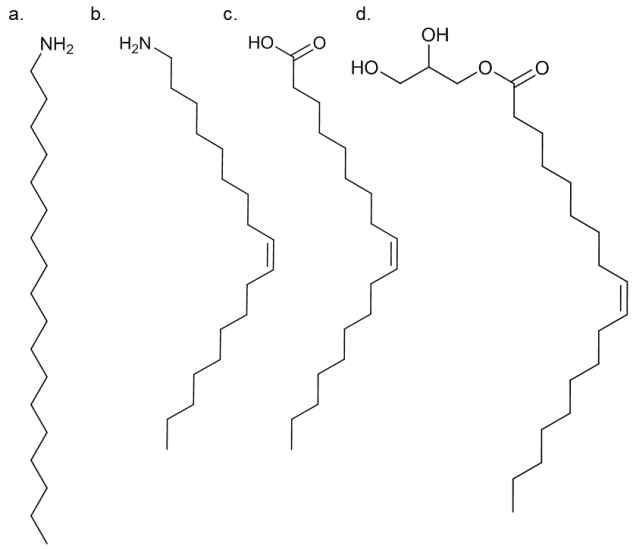

Figure 1. The structures of the OFM molecules tested, (a) octadecylamine, (b) oleylamine, (c) oleic acid, (d) glycerol monooleate (GMO)

Silicon wafers (100 orientation), used for friction and ellipsometry measurements, were purchased from Pi KEM. Borosilicate 6 mm glass balls for friction measurements were purchased from PCS instruments. SiO_2 sputter coated QCM crystals were purchased from q-sense. Analar toluene (≥ 99.5%), analar isopropanol (≥ 99.5%), analar acetone (≥ 99.5%) and hexane (99%), for cleaning and rinsing, were all purchased from Sigma Aldrich and were used as received.

EXPERIMENTAL METHODS

Friction measurements

Si wafers were cut to size of 15×15 mm^2 and cleaned in the same way as the ball, by using toluene in an ultrasonic bath for 30 minutes. These were then dried and then cleaned with oxygen plasma for 2 minutes before being assembled into the holders for the ball and disk.

Friction tests were carried out with a CETR Universal Mechanical Tester (CETR-UMT-2). The rubbing contact consisted of a stationary glass ball against a rotating silicon wafer. At the start of the test, 2 mL of lubricant was injected, flooding the contact. The ball and the disk remained stationary for 2 minutes to allow the OFM adsorbed layer to form. The test was then carried

out with an applied load of 5 N, giving an average Hertzian pressure of 0.72 GPa. The sliding speed at the contact was 1 mm/s. As a result, the estimated Hertzian minimum film thickness[21] is 12 nm, which is smaller than the roughness of the ball <50 nm. Therefore the rubbing contact was lubricated in the boundary lubrication regime. The radius of the disc rotation was 1 mm, thus each disc rotation corresponded to a sliding distance of 6.28 mm. A total sliding distance per test was 628 mm (100 rotations). All tests were carried out at room temperature (23-27 °C). Each result is an average of 4 measurements. Note that data from the 1st to the 5th rotation are instantaneous friction coefficients while data after the 5th rotation (see Figure S1 and Figure S3) are running averages at 1-rotation intervals.

Rubbed disks were rinsed with hexane and the morphology of the wear tracks were examined using a Veeco scanning white light interferometer.

Ellipsometry

Ellipsometry is a laser based technique used for measuring the optical properties of a surface.[22] It has been used to measure the thickness of surfactant monolayers on gold[23,24] and silicon[25,26] surfaces; and adsorption kinetics and surface layer thicknesses in-situ of many systems, such as proteins[27,28] and polymers[29] in aqueous systems. Ellipsometry has also been applied to quantify the thickness of a ZDDP tribofilm,[30] as well as the thickness of DLC coatings[31] and MoS_2 layers in air.[32] Within a sliding contact lubricated with a base oil, ellipsometry has been used to measure in situ the oil film thickness between the two surfaces with nm accuracy.[33] Ellipsometry has yet to be applied to examine the adsorption of additives in oil lubricated contacts. This is because base oils and OFM additives have similar refractive indices, which are 1.43 and 1.46 respectively. Note also that most ellipsometry experiments were conducted with flat, well characterised surfaces such SiO_2 surface, rather than commonly used metal surfaces such as steel, which are rougher and with less well defined refractive index.

In this study, an Accurion Nanofilm EP3 imaging ellipsometer[34] with a solid-liquid cell attachment was used. The ellipsometer has a PCSA (Polariser, Compensator, Surface and Analyser) setup. In this setup, an elliptically polarised light, which was created by passing light through a polariser, then through a quarter wavelength compensator (fixed at 45°), was directed to the sample. The light reflected off the sample surface was collected through a 10× objective, which then passed through an analyser before it was captured by a CCD camera. The measurements were based on nulling ellipsometry.[34,22] Briefly, ellipsometry measures the complex reflection coefficient of the light reflected off a surface. With the incident angle and wavelength of the incident light known, the ratio of the reflected parallel (R_p) and perpendicular (R_s) polarised light is related to values Ψ and Δ using Equation (1). This is practically measured at the null point by the angles of the polariser θ_p, and the analyser θ_a. Ψ and Δ were then calculated from: θ_p, θ_a.[22]

$$\frac{R_p}{R_s} = \tan(\Psi)e^{i\Delta} \quad (1)$$

An optical model (Figure 2), which consisted of an adsorbed layer on top of a silicon oxide (SiO_2) layer, was created. The refractive indices and film thicknesses of individual layers were then varied. Modelling of the reflected surface was carried out using Accurion's EP4 modelling software. The model is deemed to represent the surface properties of the sample when the values of Ψ and Δ obtained from the model matched the experimental values. The refractive indices of 100 Si and SiO_2, which change with the incident wavelength, were used as provided in the fitting software. The Cauchy model [22] was used for the refractive index of hexadecane based on a measurement at the air-hexadecane interface. A fixed refractive index of 1.55 was used for the adsorbed layer of all OFM additives. This was calculated from calibration tests as explained in the supporting information (S1) and was in agreement with the refractive indices of organosilane monolayers of 1.43 – 1.58[35] stated in the literature.

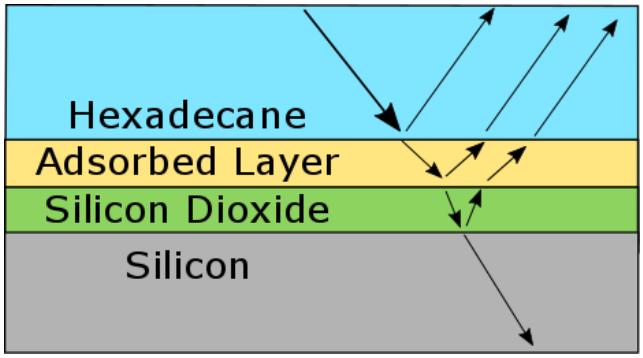

Figure 2. The optical model used to fit Ψ & Δ to calculate the thickness of the adsorbed layer in hexadecane.

Two types of ellipsometry measurements were conducted, with the angle of laser incidence set at 60°. Spectroscopic (SE) measurements, which took an hour to run, were performed with 40 different wavelengths from 371-1000 nm. Four zone averaging, with combinations of both positive and negative angles of the polariser (P) and analyser (A), and the quarter waveplate compensator (C, fixed at 45°) (+P, +A, +C; +P, +A –C; -P, -A, +C; and –P, -A, –C), was used for each value of Ψ and Δ to remove any systematic errors[22]. Kinetic measurements used a 552.2 nm light source, with Ψ and Δ recorded every 10 seconds, using only the condition of +P, +A and +C. Note that the area examined during each measurement was about 500 × 1000 μm^2.

A piece of Si wafer (25 × 10 mm^2) was cleaned with toluene and oxygen plasma, in a similar way to those for friction tests. A SE measurement was used to characterise the thickness of SiO_2 on the surface in air, which ranged from 20-50 Å. The Si wafer was then placed in the liquid cell filled with hexadecane. Without fluid flow, a kinetic measurement was undertaken to check the Ψ and Δ values. When these values were stable, a SE measurement was performed to measure the thickness of any adsorbed layer on the Si wafer, which showed no adsorbed film. With hexadecane flowing at 1 ml/min, a kinetic measurement was performed for 10 mins to check the stability of Ψ and Δ values. Once they were stable, a kinetic measurement was performed with the OFM solution flowing into the liquid cell at 1 ml/min to allow OFM to

adsorb on the Si wafer. The adsorption period was 2 hours (see Figure S1b and Figure S3b), after which the flow was stopped. A SE measurement was conducted to measure the thickness of the adsorbed layer more accurately. The thickness of the OFM adsorbed layer is taken as the difference in thickness of the adsorbed layer obtained in hexadecane and that in OFM solution. The first 30 mins of the adsorption process is shown in Figures 3 and 5 for clarity.

Results presented are average of at least two tests. The kinetic measurements shown are representative of the behaviour of each OFM solutions.

Quartz Crystal Microbalance

A QSense quartz crystal microbalance with dissipation (QCM-D) was used to measure the mass and the properties of the OFM adsorbed film. A QCM measures the resonance frequency f of a SiO_2 coated quartz crystal, which may drop as molecules deposit onto its surface. The dissipation of the crystal D is defined as the ratio of energy loss to that of the elastic energy input and may change depending on the properties of the adsorbed layer.[36] The resonance frequency of the quartz crystal used in this study is 5 MHz in air. The relationship between the adsorbed mass (Δm) and the change in resonance frequency (Δf) is described by the Sauerbrey equation, Equation (2) [37]. Note that C is related to the properties of the quartz crystal and in our case = 17.7 mg/m^2 and O is the harmonic overtone number. Equation (2) assumes that the adsorbed layer is relatively rigid (as shown by $\Delta D \sim 0$), and the adsorbed layer is uniform over the surface of the crystal.

$$\Delta m = \frac{C\Delta f_O}{O} \qquad (2)$$

A QCM crystal was rinsed with toluene and isopropanol before UV Ozone cleaning for 30 minutes. The resonance frequencies and dissipations of the various odd overtones (O: 1 - 13) were measured in air before hexadecane was injected at a flow rate of 0.35 ml/min at 20°C. Once a stable baseline was obtained, the OFM solution at the same flow rate was added for 2

hours. To obtain the adsorbed OFM mass, data is corrected to take into account the differences in densities and viscosities of pure hexadecane and OFM solutions (see Table S1).[38] The adsorbed mass is recorded over the full 2 hours of adsorption (see Figure S1a and Figure S3a). Tests were also run at a faster flow rate, which gave similar results, showing that the adsorption was not transport limited. The change in the adsorbed mass on the surface over time for the first 30 minutes is shown in Figures 3 and 5 for clarity. At least two tests were conducted for each OFM solutions.

Comparing Results from QCM and Ellipsometry

Since both QCM and ellipsometry examine the adsorption behaviour of OFMs, their results should be related. They are linked most often using De Feijter's equation, which uses the change in refractive index with concentration ($\frac{dn}{dc}$) to correlate adsorbed film thickness with surface excess.[39] This works well for protein adsorption in aqueous solutions where $\frac{dn}{dc}$ is large. For OFMs in hexadecane, however where $\frac{dn}{dc}$ is ten times smaller than that of protein in aqueous solutions, the error incurred using De Feijter's equation can be substantial. In this case, the Cuypers method as shown in Equation (3)[27] may be used. To convert the thickness of the adsorbed layer (d) to the mass adsorbed on the surface (m), the density of the layer is required (ρ^o). The density is estimated by the ratio of the molecular weight (M) to the molar refractivity (A) of a molecule, along with the specific volume of the OFM (V_{20}) and the refractive indices of the pure OFM (n) and pure solvent (n_{amb}).

$$m = d.\rho^o = \frac{0.3}{\frac{A}{M} - V_{20}\frac{n_{amb}^2-1}{n_{amb}^2+2}} * \frac{n+n_{amb}}{(n^2+2)(n_{amb}^2+2)} * d(n-n_{amb}) \qquad (3)$$

The Cuyper's method shown in Equation (3) was used to compare the results obtained from QCM to ellipsometry measurements. Values of parameters in Equation (3) can be found in supporting information, Table S2.

RESULTS AND DISCUSSION

Change of OFM additive structure

The four OFMs chosen in this study, octadecylamine, oleylamine, oleic acid and glycerol monooleate, have different structures, as shown in Figure 1. Octadecylamine and oleylamine are straight and bent chained molecules respectively with amine head groups; oleic acid and glycerol monooleate are bent chained molecules with a carboxylic acid and a glycerol ester head groups respectively. They adsorb onto the SiO_2 surface to different extents, as shown in Figure 3. The adsorbed mass of the OFM detected by the QCM measurements (Figure 3a) show that as soon as the OFM solutions are injected into the flow cell (at time = 0), a large initial adsorption onto the SiO_2 surface is observed. For all OFMs, the rates of adsorption decrease and then stabilise at much lower rates within 10 mins. The rate of decrease in the adsorption rate depends on the structure of the OFM. After 30 minutes of adsorption (and the same after 2 hours as shown in Figure S1), oleic acid (orange circles) adsorbs the least on the SiO_2 surface followed by oleylamine (red diamonds). 1 mM GMO (black inverted triangles) results in higher adsorbed mass compared to the other unsaturated OFMs. This may be partly due to its higher molecular weight. The straight chained octadecylamine (blue squares) results in the highest adsorbed mass, which stabilises quickly.

When OFM solutions are injected into the liquid cell during kinetic ellipsometry measurements, Δ drops, with the greatest reduction in Δ occurs immediately after the injection of OFM solutions (Figure 3b). Note that a reduction in Δ is related to an increase in adsorbed film thickness. Octadecylamine (blue squares) forms the thickest films with oleic acid (orange circles) the thinnest. Oleylamine (red diamonds) gives a slightly thicker film than oleic acid.

Its change in Δ is around 1/4 of that of octadecylamine film, similar to what is observed in terms of adsorbed mass with QCM experiments. In general, changes in OFM adsorbed film thicknesses, as shown in kinetic ellipsometry measurements (Figure 3b), confirm results from QCM measurements. The most noticeable difference between the QCM and ellipsometry results is the adsorption behaviour of the 1 mM GMO solution (black inverted triangles) which shows a similar change in Δ to oleylamine (red diamonds).

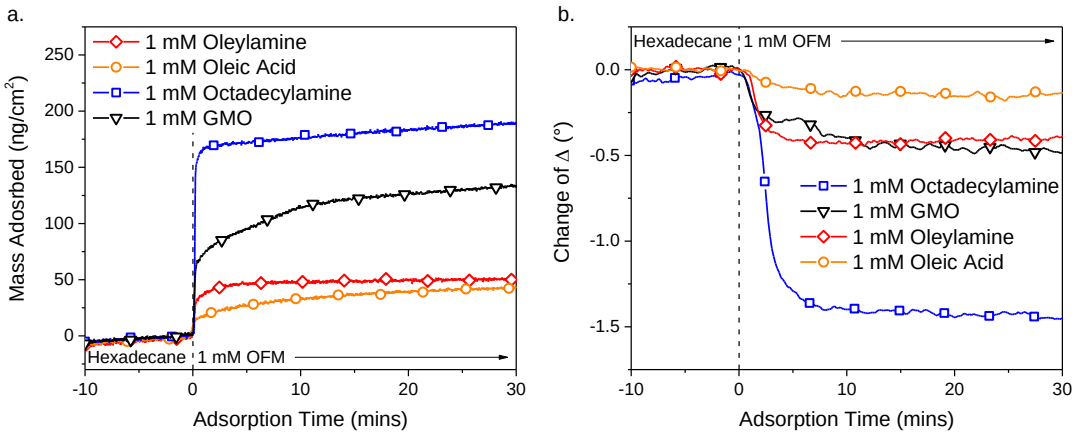

Figure 3. The adsorption of 1 mM OFM additives from hexadecane on SiO_2 examined with (a) QCM; and (b) ellipsometry. Injection of OFM solution at adsorption time = 0.

The effect of OFM additives in hexadecane on the friction of glass-silicon contacts is shown in Figure 4. There is a clear difference in the friction coefficients of these five solutions during the first rotation of rubbing: pure hexadecane (green triangles) and 1 mM oleic acid solution (orange circles) have similarly high friction coefficients. The solutions of 1 mM oleylamine (red diamonds) and GMO (black inverted triangles) provide lower friction coefficients. The saturated chain of octadecylamine (blue squares) gives the lowest friction coefficient. Based on the results from QCM and ellipsometry experiments, OFMs that adsorb more quickly result in lower friction coefficients at the first rotation.

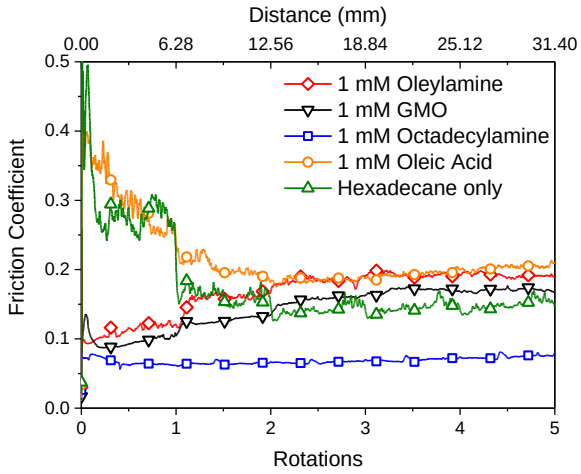

Figure 4. The friction coefficients of different OFM solutions in a glass on Si contact.

After the first rotation, the friction coefficient of 1 mM octadecylamine (blue squares) remains constant in the first 5 rotations. Changes in friction coefficients are however observed for all other solutions, particularly 1 mM oleic acid (orange circles) and neat hexadecane (green triangles). At the 100th rotations (see Figure S2), all solutions have friction coefficients within the range of 0.1 to 0.15, with all OFM solutions have a lower friction coefficient than neat hexadecane.

Change of additive concentration

The amount the additive adsorbs onto the surface may change with the concentration of the additive in the solution, as shown in Figure 5 for oleylamine. Both QCM and ellipsometry measurements show that the initial adsorbed mass of oleylamine increases with its concentration. The 0.1 mM solution (pink stars) has the slowest initial adsorption kinetics although after 30 minutes, its adsorbed layer has similar mass and thickness to those of 1 mM oleylamine (red triangles).

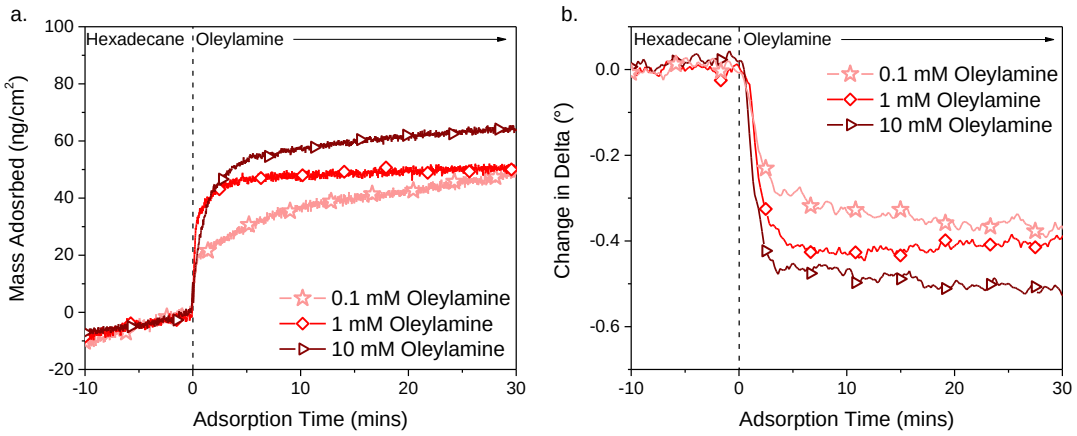

Figure 5. The change in adsorption of 10, 1 and 0.1 mM of oleylamine solution on SiO_2 surface as measured through a) QCM and b) ellipsometry. Injection of OFM solution at adsorption time = 0.

The concentration of OFM affects the friction reduction properties of the solution as shown in Figure 6. For the first rotation, 0.1 mM oleylamine (pink stars) only provides a slight friction reduction compared to neat hexadecane (green triangles). Increasing OFM concentration gives a lower friction coefficient during the first rotation only. These results support that OFM adsorption governs initial friction behaviour. At the 100th rotations (see Figure S4), all solutions have friction coefficients within the range of 0.12 to 0.15.

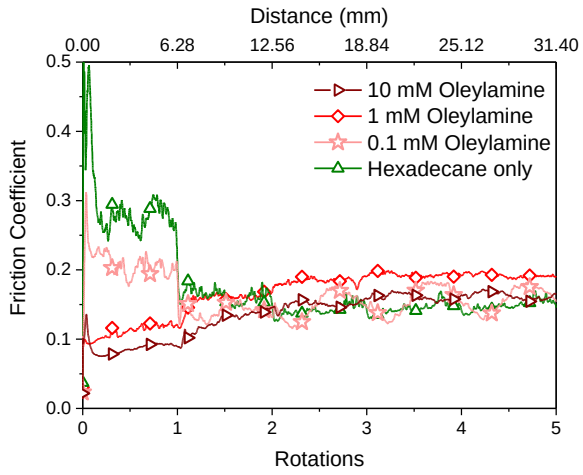

Figure 6. The change in friction reducing properties of Oleylamine at different concentrations in a Glass on Si contact.

Wear of the disk

Wear tracks on the silicon wafers after 100 rotations of rubbing were examined through scanning white light interferometry (as shown in Figure S5). The amount of surface damage is characterised by the width of the wear tracks, shown in Figure 7. The lower the initial friction, the smaller the width of the wear track (Figure 7a). Interestingly this trend is not observed for the steady state friction acquired at 100th rotation as shown in Figure 7b.

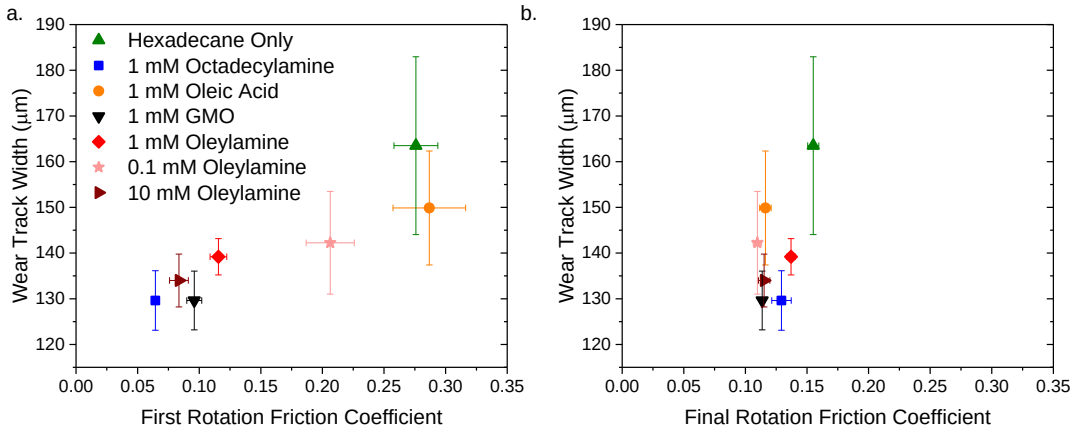

Figure 1. The correlation between the width of the wear track on the Si wafer and the a) friction of the first rotation, b) friction of the 100th rotation.

Using ellipsometry for OFM adsorption kinetics in hexadecane

Both the ellipsometry and the QCM experiments show oleic acid, oleylamine, octadecylamine and GMO in hexadecane adsorb on silicon wafer to various extent. The thickness of the OFM layer on the QCM crystal after an adsorption time of 10 minutes can be estimated by its adsorbed mass using Cuyper's method (Equation (3)). This matches that from ellipsometry reasonably well, as shown in Figure 8. A similar conclusion can also be made after an adsorption time of 2 hours (see Figure S6). This shows that spectrometric ellipsometry can provide useful information on OFM adsorption in organic solvents where the solvents and the pure additives have similar refractive indices.

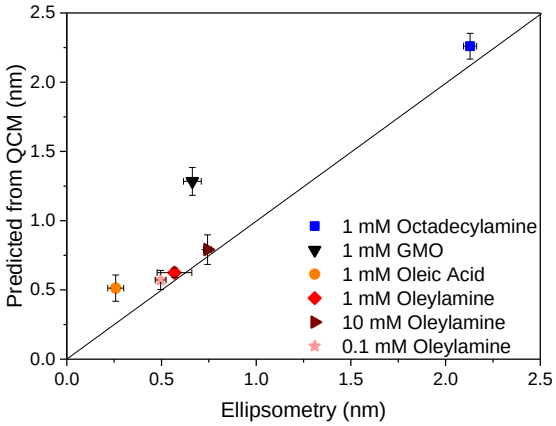

Figure 8. Comparison of adsorbed film thickness on SiO_2 obtained from QCM and ellipsometry measurements. Adsorption time = 10 minutes.

The outlier after 10-minute adsorption time in Figure 8 is 1 mM GMO (black inverted triangle), with its thickness estimates from QCM results higher than that from the ellipsometry. Interestingly, 0.1 mM oleylamine (pink Stars, Figure S3) also shows a greater adsorption height from the QCM measurements than the ellipsometry measurements after a 2-hour adsorption time. This height, as measured with QCM, is also greater than that of 1 mM oleylamine, which is contrary to the expected adsorption isotherm where the adsorbed mass should increase with concentration.[40] It has been suggested that QCM measures the true sensed mass, whereas ellipsometry would measure the adsorbed mass.[19] Assuming a uniform layer with a fixed refractive index, the true sensed mass would include the mass of the trapped solvent in the adsorbed layer, whereas the adsorbed mass would only measure the averaged amount of OFM on the surface. It is possible that when the concentration of the OFM solution is low (as in the case of 0.1 mM oleylamine) or due to the molecular structure of the OFM (as for GMO), a higher fraction of the adsorbed layer is made of trapped solvent, perhaps due to its low relative packing density.[41] As a result, the OFM adsorbed layer may appear thicker from the QCM measurement. Since GMO is more polar than other OFMs tested, polar contaminants such as water may also be incorporated into the adsorbed layer more readily.

Linking adsorption and friction properties of OFM

The relationship between the friction coefficient of the first rotation given by these OFM layers and the thicknesses of their surface adsorbed layers after 10 min is shown in Figure 9 (for results based on the thickness of OFM adsorbed layer after 2 hours of adsorption, see Figure S7). In this study the thinnest adsorbed layers are formed with 0.1 mM oleylamine (pink stars) and 1 mM oleic acid (orange circles) and are around 0.2 – 0.5 nm. They result in high friction ($\mu > 0.2$). When the adsorbed OFM layer reaches a critical height of about 0.6 nm, which is the case for 1 mM oleylamine (red diamonds) and 1 mM glycerol monooleate (black inverted triangles), μ is around 0.1. Further increase in the adsorbed film thickness only has a very small effect on friction reduction, as seen with 1 mM octadecylamine (blue squares) which has a thickness of about 2.2 nm and μ is around 0.065. The results in Figure 9 suggest that the thickness of the adsorbed layer influences the friction coefficient of the first rotation in boundary lubrication regime.

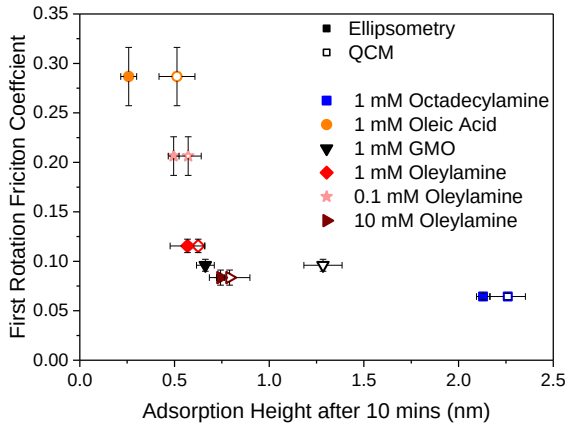

Figure 9. The relationship between the thicknesses of adsorbed layers of different OFM additives after 10 minutes of adsorption through QCM (open symbols) and ellipsometry (closed symbols) and the friction coefficient of the first rotation.

The adsorbed film thickness is governed by the chain length and the surface coverage of OFM, with the latter related to head group chemistry, molecular structure and bulk concentrations.

Indeed octadecylamine, which is a fully saturated straight chain molecule that can be packed densely easily, have the thickest layer while the adsorbed layer that are formed by low concentration OFM solution has the thinnest film. Assuming that the OFM adsorbed layers are monolayers, the surface area occupied by an OFM molecule can be estimated, as shown in Figure 10. For these conditions a critical surface OFM density could be found at around 100 $Å^2$/molecule. This value represents tail densities and is suggested to be linked to an increased van der Waals forces in the monolayer.[7] Films more densely packed than 100 $Å^2$/molecule provide a slight reduction on the friction coefficient.

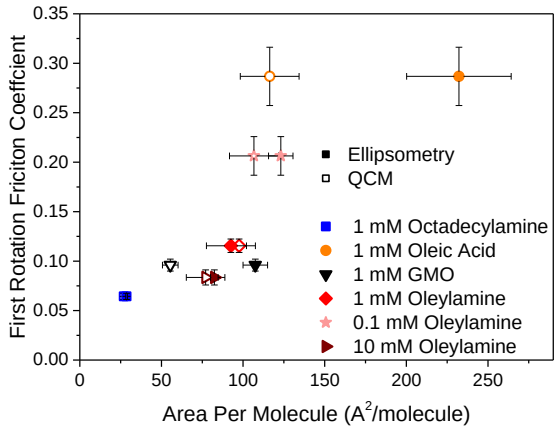

Figure 10. The relationship between OFM surface densities at 10 minutes adsorption time as calculated through results by QCM (open symbols) and ellipsometry (closed symbols) and the friction reduction of the first rotation. Results based on 2-hour adsorption time is in Figure S8.

The discussion so far has focused on the initial friction observed during the first rotation of the friction test. Except for 1 mM octadecylamine which has a densely packed adsorbed layer on the surface, the friction coefficients for other OFM solutions change within the first 5 rotations. By the 100th rotation, all additives have a steady state values of about $\mu = 0.11 – 0.15$ (see Figure S2), which is lower than that of neat hexadecane. Note that the thicknesses of OFM adsorbed layers observed in QCM and ellipsometry measurements does not change substantially with time (see Figure S1 for data after adsorption for 2 hours). This suggests that

factors other than surface adsorption may play a role in determining steady state friction coefficients.

The surface of a silicon wafer, used as the rubbing surface in this study, has a thin layer of SiO_2 (20-50 Å). During the run-in period, the SiO_2 layer may be removed during rubbing, resulting in a pure Si surface instead.[42] Hence the friction coefficient may change as the interaction of the OFMs with the Si surface may be different to that with SiO_2. Note the parameters used for the optical model (as described in Figure 2) cannot be used to fit surface properties of wear track successfully. This provides qualitative support that the surface properties of the silicon wafer are altered due to rubbing. Sliding may also alter the structure of the adsorbed surface layer through shear removal, molecular ordering, or pressure induced multilayer formation as hypothesised by Hirayama et al.[18] Tribochemistry may also be a factor in this change of friction coefficient. For example, GMO has thought to potentially hydrolyse to form oleic acid within a sliding contact[1] or even break down further as it does on Ta-C DLC coatings.[43] Our observations are most likely due to a combination of these factors.

The friction coefficient of the first rotation, as shown in Figure 7, is positively correlated to the wear track width, as well as the maximum friction coefficient experienced during the friction test, see Figure S9. Our results show that an increase in wear track width, signifies increased wear, is linked to the maximum friction coefficient of the tribopair. Interestingly, the wider wear tracks, as observed with thinner OFM layers, have lower surface roughness (see Figure S10). This may be due to the better protection provided by thicker OFM layers, preserving the rougher surface topography of the ball produced when friction is the highest.

CONCLUSIONS

In this work, ellipsometry and quartz crystal microbalance were used to examine the adsorption of OFM additives on silicon in hexadecane. The results were then correlated with the effectiveness of OFM in reducing friction in a glass-silicon contact under the boundary lubricant regime.

We show that ellipsometry is a suitable technique for measuring the growth of OFM films in oil based solutions on smooth surfaces of SiO_2. These results match those obtained through a quartz crystal microbalance relatively well. Depending of the molecular structures of OFMs, OFM layers differ in thicknesses and hence their surface coverage.

The properties of OFM adsorbed layers govern the initial friction of a glass-silicon rubbing pair. Octadecylamine forms a thick layer that leads to low initial friction while thin oleic acid layers and oleylamine layers result in high friction. GMO forms an adsorbed layer of intermediate thickness even though its friction coefficient is comparable to that of octadecylamine. These results suggest a critical thickness of about 0.6 nm is necessary to provide low initial friction. Note that rougher test surfaces or more severe contact conditions may require higher critical thickness for effective OFM layers.

The thicker OFM layers result in narrower, rougher wear tracks than the wider, smoother tracks observed with thinner OFM layers. It is likely that the roughness of wear track changes as rubbing progresses and a wear track is at its roughest when the maximum friction is achieved. Since the thinner OFM layers are linked to a higher maximum friction, it is possible at the time the maximum friction is reached, the wear track associated with thinner OFM layers are rougher. The thicker OFM layer may however be better in preserving the surface topography: as such, after 100 rotations of rubbing, the wear track with the thinner OFM layer is smoother than that with thicker OFM film. The differences in surface roughness counter the effect of the properties of OFM layer on the wear track which eventually lead to all OFMs giving similar

friction coefficients at the 100th rotation. This shows that the impact of the properties of OFM adsorbed layers extend beyond the initial friction to the subsequent surface damage.

AUTHOR INFORMATION

Corresponding author

†Janet S. S. Wong j.wong@imperial.ac.uk

Author Contributions

All authors have given approval to the final version of the manuscript.

Funding Sources

B.F. is financially supported by Croda Europe Ltd and the EPSRC (EP/N509486/1).

ACKNOWLEDGEMENTS

B.F. is financially supported by Croda Europe Ltd and the EPSRC (EP/N509486/1). We would like to thank Prof Tony Cass for the use of spectroscopic ellipsometry and Dr Sophie Campen for her help in quartz crystal microbalance.

ABBREVIATIONS

OFM, organic friction modifiers; QCM, quartz crystal microbalance; SAMs, self-assembled monolayers; GMO, glycerol monooleate; SE, Spectroscopic ellipsometry

SUPPORTING INFORMATION

S1 The description of the OFM monolayer refractive index.

Table S1 The densities and viscosities of the OFM solutions.

Table S2 The values used for the Cuypers method.

Figure S1 Adsorption of different OFM additives after 2 hours

REFERENCES

(1) Spikes, H. Friction Modifier Additives. *Tribol. Lett.* **2015**, *60* (1), 5–30. https://doi.org/10.1007/s11249-015-0589-z.

(2) Langmuir, I. The Mechanism of the Surface Phenomena of Flotation. *Trans. Faraday Soc.* **1920**, *15*, 62–74. https://doi.org/10.1039/TF9201500062.

(3) Hardy, W. B.; Doubleday, I. Boundary Lubrication-the Paraffin Series. *Proc. R. Soc. Lond. A.* **1922**, *100* (707), 550–557. https://doi.org/10.1098/rspa.1983.0054.

(4) Schreiber, F. Structure and Growth of Self-Assembling Monolayers. *Prog. Surf. Sci.* **2000**, *65* (5–8), 151–256. https://doi.org/10.1016/S0079-6816(00)00024-1.

(5) McDermott, M. T.; Green, J.-B. D.; Porter, M. D. Scanning Force Microscopic Exploration of the Lubrication Capabilities of n -Alkanethiolate Monolayers Chemisorbed at Gold: Structural Basis of Microscopic Friction and Wear. *Langmuir*

2002, *13* (9), 2504–2510. https://doi.org/10.1021/la962099m.

(6) Lee, S.; Shon, Y. S.; Colorado, R.; Guenard, R. L.; Lee, T. R.; Perry, S. S. Influence of Packing Densities and Surface Order on the Frictional Properties of Alkanethiol Self-Assembled Monolayers (SAMs) on Gold: A Comparison of SAMs Derived from Normal and Spiroalkanedithiols. *Langmuir* **2000**, *16* (5), 2220–2224. https://doi.org/10.1021/la9909345.

(7) Salmeron, M. Generation of Defects in Model Lubricant Monolayers and Their Contribution to Energy Dissipation in Friction. *Tribol. Lett.* **2001**, *10* (1–2), 69–79. https://doi.org/10.1023/A:1009026312732.

(8) Hardy, W. B.; Doubleday, I. Boundary Lubrication. The Paraffin Series. *Proc. R. Soc. Lond. A.* **1922**, *101* (709), 169–174. https://doi.org/10.1098/rspa.1983.0054.

(9) Jahanmir, S. Chain Length Effects in Boundary Lubrication. *Wear* **1985**, *102* (4), 331–349. https://doi.org/10.1016/0043-1648(85)90176-0.

(10) Lundgren, S. M.; Persson, K.; Mueller, G.; Kronberg, B.; Clarke, J.; Chtaib, M.; Claesson, P. M. Unsaturated Fatty Acids in Alkane Solution: Adsorption to Steel Surfaces. *Langmuir* **2007**, *23* (7), 10598–10602. https://doi.org/10.1021/1a70090v.

(11) Nalam, P. C.; Pham, A.; Castillo, R. V.; Espinosa-Marzal, R. M. Adsorption Behavior and Nanotribology of Amine-Based Friction Modifiers on Steel Surfaces. *J. Phys. Chem. C* **2019**, *123* (22), 13672–13680. https://doi.org/10.1021/acs.jpcc.9b02097.

(12) Eder, S. J.; Vernes, A.; Betz, G. On the Derjaguin Offset in Boundary-Lubricated Nanotribological Systems. *Langmuir* **2013**, *29* (45), 13760–13772. https://doi.org/10.1021/la4026443.

(13) Doig, M.; Warrens, C. P.; Camp, P. J. Structure and Friction of Stearic Acid and Oleic

Acid Films Adsorbed on Iron Oxide Surfaces in Squalane. *Langmuir* **2014**, *30* (1), 186–195. https://doi.org/10.1021/la404024v.

(14) Ewen, J. P.; Gattinoni, C.; Morgan, N.; Spikes, H. A.; Dini, D. Nonequilibrium Molecular Dynamics Simulations of Organic Friction Modifiers Adsorbed on Iron Oxide Surfaces. *Langmuir* **2016**, *32* (18), 4450–4463. https://doi.org/10.1021/acs.langmuir.6b00586.

(15) Ewen, J. P.; Echeverri Restrepo, S.; Morgan, N.; Dini, D. Nonequilibrium Molecular Dynamics Simulations of Stearic Acid Adsorbed on Iron Surfaces with Nanoscale Roughness. *Tribol. Int.* **2017**, *107*, 264–273. https://doi.org/10.1016/j.triboint.2016.11.039.

(16) Jaishankar, A.; Jusufi, A.; Vreeland, J. L.; Deighton, S.; Pellettiere, J.; Schilowitz, A. M. Adsorption of Stearic Acid at the Iron Oxide/Oil Interface: Theory, Experiments, and Modeling. *Langmuir* **2019**, *35* (6), 2033–2046. https://doi.org/10.1021/acs.langmuir.8b03132.

(17) Hirayama, T.; Kawamura, R.; Fujino, K.; Matsuoka, T.; Komiya, H.; Onishi, H. Cross-Sectional Imaging of Boundary Lubrication Layer Formed by Fatty Acid by Means of Frequency-Modulation Atomic Force Microscopy. *Langmuir* **2017**, *33* (40), 10492–10500. https://doi.org/10.1021/acs.langmuir.7b02528.

(18) Hirayama, T.; Maeda, M.; Sasaki, Y.; Matsuoka, T.; Komiya, H.; Hino, M. Growth of Adsorbed Additive Layer for Further Friction Reduction. *Lubr. Sci.* **2019**, *31* (5), 171–178. https://doi.org/10.1002/ls.1420.

(19) Lundgren, S. M.; Persson, K.; Kronberg, B. T.; Claesson, P. M. Adsorption of Fatty Acids from Alkane Solution Studied with Quartz Crystal Microbalance. *Tribol. Lett.* **2006**, *22* (1), 15–20. https://doi.org/10.1007/s11249-005-9000-9.

(20) Wood, M. H.; Welbourn, R. J. L.; Charlton, T.; Zarbakhsh, A.; Casford, M. T.; Clarke, S. M. Hexadecylamine Adsorption at the Iron Oxide-Oil Interface. *Langmuir*. 2013, pp 13735–13742. https://doi.org/10.1021/la4018147.

(21) Hamrock, B. J.; Dowson, D. Isothermal Elastohydrodynamic Lubrication of Point Contacts - 3. Fully Flooded Results. *Am. Soc. Mech. Eng.* **1976**, No. 76-Lub-30, 264–275.

(22) Tompkins, H. G. *Handbook of Ellipsometry*; Tompkins, H. G., Irene, E. A., Eds.; Springer Berlin Heidelberg, 2005; Vol. 30. https://doi.org/10.1007/3-540-27488-X.

(23) Bain, C. D.; Troughton, E. B.; Tao, Y. T.; Evall, J.; Whitesides, G. M.; Nuzzo, R. G. Formation of Monolayer Films by the Spontaneous Assembly of Organic Thiols from Solution onto Gold. *J. Am. Chem. Soc.* **1989**, *111* (1), 321–335. https://doi.org/10.1021/ja00183a049.

(24) Nuzzo, R. G.; Allara, D. L. Adsorption of Bifunctional Organic Disulfides on Gold Surfaces. *J. Am. Chem. Soc.* **1983**, *105* (13), 4481–4483. https://doi.org/10.1021/ja00351a063.

(25) Wasserman, S. R.; Whitesides, G. M.; Tidswell, I. M.; Ocko, B. M.; Pershan, P. S.; Axel, J. D. The Structure of Self-Assembled Monolayers of Alkylsiloxanes on Silicon: A Comparison of Results from Ellipsometry and Low-Angle X-Ray Reflectivity. *J . Am. Chem. SOC* **1989**, *1* (1), 5852–5861. https://doi.org/10.1021/ja00197a054.

(26) Eskilsson, K.; Yaminsky, V. V. Deposition of Monolayers by Retraction from Solution: Ellipsometric Study of Cetyltrimethylammonium Bromide Adsorption at Silica−Air and Silica−Water Interfaces. *Langmuir* **1998**, *7463* (4), 2444–2450. https://doi.org/10.1021/la971066j.

(27) Cuypers, P. A.; Corsel, J. W.; Janssen, M. P.; Kop, J. M.; Hermens, W. T.; Hemker, H. C. The Adsorption of Prothrombin to Phosphatidylserine Multilayers Quantitated by Ellipsometry. *J. Biol. Chem.* **1983**, *258* (4), 2426–2431.

(28) Van Der Meulen, S. A. J.; Dubacheva, G. V.; Dogterom, M.; Richter, R. P.; Leunissen, M. E. Quartz Crystal Microbalance with Dissipation Monitoring and Spectroscopic Ellipsometry Measurements of the Phospholipid Bilayer Anchoring Stability and Kinetics of Hydrophobically Modified DNA Oligonucleotides. *Langmuir* **2014**, *30* (22), 6525–6533. https://doi.org/10.1021/la500940a.

(29) Gilchrist, V. A.; Lu, J. R.; Keddie, J. L.; Staples, E.; Garrett, P. Adsorption of Penta(Ethylene Glycol) Monododecyl Ether at the Solid Poly(Methyl Methacrylate)-Water Interface: A Spectroscopic Ellipsometry Study. *Langmuir* **2000**, *16* (2), 740–748. https://doi.org/10.1021/la9906572.

(30) Miranda-Medina, M. L.; Spiller, S.; Vernes, A.; Jech, M. Spectroscopic Ellipsometry and X-Ray Photoelectron Comparative Studies of Tribofilms Formed on Cast Iron Surfaces. *Tribol. Int.* **2017**, *113* (July 2016), 101–110. https://doi.org/10.1016/j.triboint.2016.12.021.

(31) Fourches, N.; Turban, G.; Grolleau, B. Study of DLC/Silicon Interfaces by XPS and in-Situ Ellipsometry. *Appl. Surf. Sci.* **1993**, *68* (1), 149–160. https://doi.org/10.1016/0169-4332(93)90224-Y.

(32) Li, D.; Song, X.; Xu, J.; Wang, Z.; Zhang, R.; Zhou, P.; Zhang, H.; Huang, R.; Wang, S.; Zheng, Y.; Zhang, D. W.; Chen, L. Optical Properties of Thickness-Controlled MoS2thin Films Studied by Spectroscopic Ellipsometry. *Appl. Surf. Sci.* **2017**, *421*, 884–890. https://doi.org/10.1016/j.apsusc.2016.09.069.

(33) Fukuzawa, K.; Sasao, Y.; Namba, K.; Yamashita, C.; Itoh, S.; Zhang, H. Measurement

of Nanometer-Thick Lubricating Films Using Ellipsometric Microscopy. *Tribol. Int.* **2018**, *122* (February), 8–14. https://doi.org/10.1016/j.triboint.2018.02.016.

(34) Asinovski, L.; Beaglehole, D.; Clarkson, M. T. Imaging Ellipsometry: Quantitative Analysis. *Phys. Status Solidi Appl. Mater. Sci.* **2008**, *205* (4), 764–771. https://doi.org/10.1002/pssa.200777855.

(35) Brunner, H.; Vallant, T.; Mayer, U.; Hoffmann, H. Formation of Ultrathin Films at the Solid-Liquid Interface Studied by in Situ Ellipsometry. *J. Colloid Interface Sci.* **1999**, *212* (2), 545–552. https://doi.org/10.1006/jcis.1998.6062.

(36) Mecea, V.; Bucur, R. V. The Mechanism of the Interaction of Thin Films with Resonating Quartz Crystal Substrates: The Energy Transfer Model. *Thin Solid Films* **1979**, *60* (1), 73–84. https://doi.org/10.1016/0040-6090(79)90349-3.

(37) Krim, J. Friction and Energy Dissipation Mechanisms in Adsorbed Molecules and Molecularly Thin Films. *Adv. Phys.* **2012**, *61* (3), 155–323. https://doi.org/10.1080/00018732.2012.706401.

(38) Kanazawa, K. K.; Gordon, J. G. The Oscillation Freguency of a Quartz Crystal Resonator in Contact with a Liquid. *Anal. Chim. Acta* **1985**, *175*, 99–105.

(39) De Feijter, J. A.; Benjamins, J.; Veer, F. A. Ellipsometry as a Tool to Study the Adsorption Behavior of Synthetic and Biopolymers at the Air- Water Interface. *Biopolymers* **1978**, *17*, 1759–1772.

(40) Atkins, P.; Paula, J. De. *Atkins' Physical Chemistry*; 2009. https://doi.org/10.1021/ed056pA260.1.

(41) Huang, L.; Shen, J.; Yu, C.; Meng, Q.; Yu, T. The Solvent Trapping or Co-Adsorbing Effect during the Self-Assembly Monolayer Studied by Surface-Enhanced Raman

Scattering. *Vib. Spectrosc.* **2001**, *25* (1), 1–5. https://doi.org/10.1016/S0924-2031(00)00100-4.

(42) Zhang, P.; Chen, C.; Xiao, C.; Chen, L.; Jiang, L.; Qian, L. Effects of Surface Chemical Groups and Environmental Media on Tribochemical Running-in Behaviors of Silicon Surface. *Tribol. Int.* **2018**, *128* (June), 174–180. https://doi.org/10.1016/j.triboint.2018.07.032.

(43) Kuwahara, T.; Romero, P. A.; Makowski, S.; Weihnacht, V.; Moras, G.; Moseler, M. Mechano-Chemical Decomposition of Organic Friction Modifiers with Multiple Reactive Centres Induces Superlubricity of Ta-C. *Nat. Commun.* **2019**, *10* (1), 151, 1–11. https://doi.org/10.1038/s41467-018-08042-8.

TOC Graphic

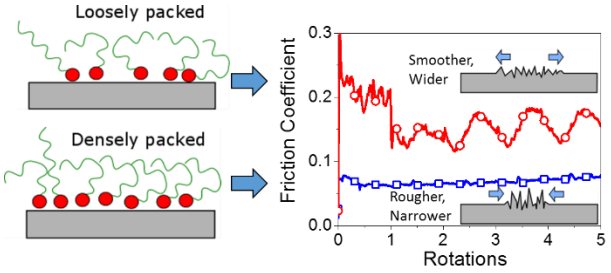
Loosely packed
Densely packed
Friction Coefficient
0.3
0.2
0.1
0.0
0
1
2
3
4
5
Rotations
Smoother,
Wider
Rougher,
Narrower